Dual-antigen targeted iPSC-derived chimeric antigen receptor-T cell therapy for refractory lymphoma

Sakiko Harada[1], Miki Ando[1,2]*, Jun Ando[1], Midori Ishii[1], Tomoyuki Yamaguchi[2], Satoshi Yamazaki[3,4], Tokuko Toyota[1], Kazuo Ohara[1], Manami Ohtaka[5], Mahito Nakanishi[5], Chansu Shin[6], Yasunori Ota[7], Kazutaka Nakashima[8], Koichi Ohshima[8], Chihaya Imai[6], Yozo Nakazawa[9], Hiromitsu Nakauchi[2,10,11]*, and Norio Komatsu[1,11]

[1] Department of Hematology, Juntendo University School of Medicine, Tokyo, Japan.
[2] Division of Stem Cell Therapy, Distinguished Professor Unit, The Institute of Medical Science, The University of Tokyo, Tokyo, Japan.
[3] Division of Stem Cell Biology, Center for Stem Cell Biology and Regenerative Medicine, The Institute of Medical Science, The University of Tokyo, Tokyo, Japan.
[4] Laboratory of Stem Cell Therapy Faculty of Medicine, University of Tsukuba, Ibaraki, Japan
[5] TOKIWA-Bio, Inc., Tsukuba Center, Ibaraki, Japan.
[6] Department of Pediatrics, Niigata University Graduate School of Medical and Dental Sciences, Niigata, Japan.
[7] Department of Pathology, Research Hospital, The Institute of Medical Science, The University of Tokyo, Tokyo, Japan.
[8]Department of Pathology, School of Medicine, Kurume University, Fukuoka, Japan.
[9] Department of Pediatrics, Shinsyu University School of Medicine, Nagano, Japan.
[10] Institute for Stem Cell Biology and Regenerative Medicine, Stanford University School of Medicine, Stanford, CA, USA.
[11] Co-senior authorship

*Correspondence:

Miki Ando, M.D., Ph.D
M.A. (m-ando@juntendo.ac.jp)
Department of Hematology, Juntendo University School of Medicine,
2-1-1 Hongo, Bunkyo-ku, Tokyo 113-8421, Japan
Phone 81-3-5802-1069

Hiromitsu Nakauchi, M.D., Ph.D.
H.N. (nakauchi@stanford.edu)
Institute for Stem Cell Biology and Regenerative Medicine
Lorry Lokey Stem Cell Research Building Room G3078B
265 Campus Drive, Stanford, CA 94305-5461, USA
Phone 1-650-497-4365

Short title: Dual-antigen targeted CTL for refractory lymphoma

Abstract

We generated dual-antigen receptor (DR) T cells from induced pluripotent stem cells (iPSC) to mitigate tumor antigen escape. These cells were engineered to express a chimeric antigen receptor (CAR) for the antigen cell surface latent membrane protein 1 (LMP1; LMP1-CAR) and a T cell receptor directed to cell surface latent membrane protein 2 (LMP2), in association with human leucocyte antigen A24, to treat therapy-refractory Epstein-Barr virus-associated lymphomas. We introduced LMP1-CAR into iPSC derived from LMP2-specific cytotoxic T lymphocytes (CTL) to generate rejuvenated CTL (rejT) active against LMP1 and LMP2, or DRrejT. All DRrejT-treated mice survived >100d. Furthermore, DRrejT rejected follow-up inocula of lymphoma cells, demonstrating that DRrejT persisted long-term. We also demonstrated that DRrejT targeting CD19 and LMP2 antigens exhibited a robust tumor suppressive effect and conferred a clear survival advantage. Co-operative antitumor effect and *in vivo* persistence, with unlimited availability of DRrejT therapy, will provide powerful and sustainable T cell immunotherapy.

Introduction

Chimeric antigen receptors (CAR) enhance effector T cell function in the tumor microenvironment. These genetically modified receptors consist of a single-chain variable fragment (scFv) as an antigen recognition module, linked to a costimulatory domain and a cytoplasmic activation domain such as the T cell receptor (TCR) CD3-ζ chain [1-5]. Relapsed and refractory acute B-lymphoblastic leukemia treated using T cells engineered to express CD19-directed CAR shows ~90% remission rates in clinical trials [6-9]. Nonetheless, relapses occur in 30% to 50% of patients because with continued T cell exposure to tumor, T cell exhaustion develops, with tumor antigen escape. This limits clinical utility [10-13]. Furthermore, CAR T cell (CART) therapy requires T cell collection, gene modification, and expansion – too long a process for some patients [14, 15].

Fully rejuvenated cytotoxic T lymphocytes (CTL) as unlimited sources of therapeutic T cells may permit "off-the-shelf" therapy. Antigen-specific CTL can be functionally rejuvenated, yielding rejuvenated CTL (rejT) by induced pluripotent stem cell (iPSC) technology [16-19] and rejT can survive long-term *in vivo* as young memory T cells [20]. In contrast, peripheral blood-derived original CTL do not prolong survival of tumor-bearing mice [20, 21].

We hypothesized that CAR and rejT in combination (dual receptor rejT; DRrejT) could overcome the drawbacks of conventional CTL as well as those of CART therapy with regard to prevention of antigen escape, persistence *in vivo*, and an unlimited cell source. DRrejT which show 100% CAR transgene expression and 100% antigen-specificity can target dual antigens, permitting the expectation that with DRrejT incidence of tumor antigen escape will be minimal. Latent membrane protein 2 (LMP2) antigen-specific rejT (LMP2-rejT) exert a strong anti-tumor effect against an aggressive and treatment-refractory lymphoma, Epstein-Barr virus (EBV)-

infected extranodal natural killer (NK)/T-cell lymphoma, nasal type (ENKL) [20]. LMP2-rejT survive >7mo in treated mice, preventing recurrence of ENKL [20]. Remarkable long-term *in vivo* persistence of LMP2-rejT also has been proven [20]. Moreover, CAR-transduced T-iPSC can efficiently produce unlimited numbers of DRrejT [18, 22].

In this report we demonstrate that DRrejT can be constructed to recognize latent membrane protein 1 (LMP1) antigen via CAR and LMP2 antigen via native TCR. In therapy, these DRrejT are superior to peripheral blood-derived LMP1-CART as well as to with LMP2-rejT: DRrejT showed 100% survival and robustly eliminated ENKL not only once but twice (initial tumor; subsequently inoculated tumor). We also generated DRrejT that recognize CD19 antigen via CAR and LMP2 antigen via native TCR to confirm the reproducibility of our results. Both DRrejT act powerfully and sustainedly against EBV-driven tumors.

Results

Lentiviral LMP1-CAR vector construction and peripheral blood LMP1-CART generation

To target LMP1$^+$ EBV-associated lymphomas, we first examined LMP1 expression of EBV-associated lymphoma cell lines. EBV-encoded small RNA (EBER) *in situ* hybridization was also conducted to detect EBV sequences. The HLA-A*2402$^+$ EBV-infected ENKL cell line NK-YS and HLA-A*2402$^+$ and A*2402$^-$ EBV-infected lymphoblastoid cell lines (LCL) expressed LMP1 and marked for EBER. The EBV-free osteosarcoma cell line HOS did not express LMP1 (Figure 1A). We next generated a lentiviral vector encoding a 3rd generation CAR directed against LMP1 antigen. The construct comprises an anti-LMP1 scFv linked to sequences encoding CD28, OX40, and CD3ζ domains (Figure 1B) [23]. The suicide gene inducible caspase-9 (iC9) is linked to LMP1-CAR via 2A-derived nucleotides to increase the safety of CART therapy

[23-25]. To confirm lentiviral LMP1-CAR vector effectiveness, we transduced peripheral blood T cells with LMP1-CAR vector. Peripheral blood mononuclear cells (PBMC) from a healthy donor were stimulated by anti-CD3 and anti-CD28 antibodies and transduced with the lentiviral LMP1-CAR vector. After 3d, the LMP1-CAR-transduced cells were stained with biotinylated protein L, which binds to scFv of CAR, followed by streptavidin- allophycocyanin (APC) staining, and measured APC positivity by flow cytometry [26]. The CAR transgene was expressed by 25.4% of LMP1-CART cells (LMP1-CART) and the percentages of $CD4^+$ and $CD8^+$ LMP1-CART were respectively 30.3% and 68.0% (Figure 1C). To verify antitumor activity of PBMC-derived LMP1-CART against LMP1-expressing tumor cells, we performed coculture experiments. PBMC-derived LMP1-CART were cocultured with EBV-infected lymphoblastoid cell lines (LCL) that express LMP1 antigen on their surfaces [27] at an effector : target ratio (E : T ratio) of 1:1. The percentages of LMP1-CART and LCL were determined 0, 5, and 7d after coculture began by flow cytometry to detect $CD3^+$ $CD19^-$ cells and $CD3^-$ $CD19^+$ cells respectively. On day 7 of coculture, activated LMP1-CART were abundant and proportions of LCL were low (LMP1-CART : LCL= 98.0% : 0.36%), whereas LCL were clearly abundant when control effector T cells (activated T cells) were cocultured with LCL (activated T cells : LCL= 17.3% : 71.6%) (Figure 1D left). At the same time, absolute cell numbers were measured using counting beads on flow cytometry. LCL cocultured with LMP1-CART decreased from 95,289 ± 10,650 (Day 0) to 47,533 ± 29,816 (Day 7). However, LCL cocultured with activated T cells rapidly increased from 132,298 ± 17,458 (Day 0) to 978,716 ± 132,325 (Day 7) (Figure 1D, right).

These results indicated that the lentiviral LMP1-CAR recognized LMP1 antigens on LCL and that activated CART suppressed the proliferation of LCL.

iPSC-derived DRrejT with 100% LMP1-CAR expression and LMP2-specific native TCR were successfully generated

We next generated iPSC-derived DRrejT (Figure 1E). LMP2 antigen-specific CTL (PYLFWLAAI) were generated from a healthy donor expressing human leucocyte antigen (HLA) A*2402. The generated LMP2-specific CTL were cloned and reprogrammed into T-iPSC with the Sendai virus vectors encoding the Yamanaka 4 factors (*OCT3/4*, *SOX2*, *KLF4*, and *c-MYC*) and SV40 large T antigen [16-18, 20]. After T-iPSC establishment, the T-iPSC were transduced with lentiviral LMP1-CAR vector [17]. To select for cells without LMP1-CAR silencing, and thus with stable CAR transgene expression, LMP1-CAR-transduced T-iPSC were repeatedly sorted for biotinylated protein L expression. After 3 sortings, LMP1-CAR-T-iPSC were differentiated into LMP1-CAR-expressing LMP2-rejT, or DRrejT (Figure 1E). To evaluate CAR transgene expression and LMP2 antigen specificity in DRrejT, biotinylated protein L staining and LMP2 tetramer analysis were conducted. CAR-specific biotinylated protein L staining was 100%, which means that CAR transgene expression in DRrejT was 100% (Figure 1F), a proportion much higher than that in PBMC-derived LMP1-CART (25.4%) (Figure 1C), suggesting that the cytotoxicity of DRrejT against LMP1-expressing tumors could be expected to be stronger than that of PBMC-derived LMP1-CART. The specificity of LMP2 antigen in DRrejT was also shown to be 99.1% by tetramer staining (Figure 1F). Furthermore, expression of programmed cell death protein 1 (PD-1), a marker of T cell exhaustion, was compared by flow cytometry with that of DRrejT and PBMC-derived LMP1-CART. The average PD-1 expression was 11.51 ± 4.92 % of PBMC-derived LMP1-CART and 0.85 ± 0.79 % of DRrejT ($p=0.0052$ by unpaired Student's *t* test) (Figure 1G).

In sum, we successfully generated iPSC-derived DRrejT that exhibited 100% expression of LMP1-CAR transgene and 99% expression of native TCR recognizing LMP2 antigen, with almost complete absence of PD-1 expression.

DRrejT exert greater cytotoxicity than LMP1-CART against ENKL

To compare the cytotoxicity of DRrejT with that of PBMC-derived LMP1-CART against NK-YS cells, we performed chromium-51 (^{51}Cr) release assays. We identified stronger cytotoxicity against NK-YS cells with DRrejT than with LMP1-CART, with specific lysis of 86.1±5.9% vs 48.2±13.6% ($p=0.0114$, unpaired Student's *t* test) and 68.3±3.1% vs 31.7±2.1% ($p<0.0001$, unpaired Student's *t* test) at E : T ratios of 5:1 and 2.5:1, respectively (Figure 2A). To compare further the *in vivo* cytotoxicity of peripheral blood-derived LMP1-CART against ENKL cells with that of DRrejT, NK-YS transduced with retroviral vector encoding a green fluorescent protein (GFP) - firefly luciferase (FFLuc) fusion protein (GFP/FFLuc) were intraperitoneally engrafted into NOD/Shi-scid, IL-2RγKO Jic (NOG) mice ($1x10^5$ cells/mouse). Bioluminescence, a signal that indicates tumor growth, was monitored. Four days after tumor injection, mice were divided into 3 groups: a no treatment group (n=5), a peripheral blood-derived LMP1-CART group (n=7), and a DRrejT group (n=8). In the two treatment groups, LMP1-CART or DRrejT were intraperitoneally injected on day 0, day 7, and day 14 ($5x\ 10^6$ per dose, 3 doses). DRrejT more rapidly yielded a continuous anti-ENKL effect. While LMP1-CART suppressed ENKL proliferation to a certain degree short-term, tumor enlargement rapidly occurred in mice treated with LMP1-CART, beginning 23d after the 1st treatment; *i.e.*, the tumor suppressive effect of LMP1-CART did not last long (Figure 2B). Accordingly, only DRrejT showed a significant

survival advantage over both the no treatment group (p=0.0001) and the peripheral blood-derived LMP1-CART group (p<0.0001 by log-rank test) (Figure 2C).

To compare the cytotoxicity against NK-YS cells of DRrejT with that of non-LMP2-specific LMP1-CAR rejT, we performed ^{51}Cr release assays. We also confirmed stronger cytotoxicity against NK-YS cells with DRrejT than with LMP1-CAR/HPV-rejT, with specific lysis of 83.1 ± 2.7% vs 40.6 ± 4.5% (p=0.0002, unpaired Student's *t* test) and 70.9 ± 7.0% vs 34.1 ± 4.2% (p=0.0014, unpaired Student's *t* test) at E : T ratios of 10:1 and 5:1, respectively (Figure 2D).

For serial killing experiments, DRrejT ($CD3^+$ and GFP^-) were cocultured with GFP/FFLuc NK-YS ($CD3^-$ and GFP^+), at an E : T ratio of 5:1. On day 5 of coculture, DRrejT had eliminated substantial numbers of NK-YS, which dropped from 8.5% (day 0) to 0.9% (day 5). By contrast, control rejT that were not specific to EBV antigen could not eliminate the target cells and allowed the proliferation of NK-YS cells which rose from 9.0% (day 0) to 14.7% (day 5) and 38.4% (day 7) (Figure 2E left). The absolute cell number of GFP/FFLuc NK-YS cocultured with DRrejT actually decreased from 94,861 ± 2,223 (Day 0) to 5,914 ± 133 (Day 7), whereas NK-YS cocultured with control rejT increased from 83,896 ± 4,987 (Day 0) to 114,119 ± 15,004 (Day 7) (Figure 2E, right).

These data indicated that DRrejT showed a tumor-suppressive effect against ENKL stronger than that of peripheral blood-derived LMP1-CART both *in vitro* and *in vivo*.

DRrejT exhibited additive killing via LMP1-CAR

To learn if DRrejT exhibit a killing effect beyond that of LMP2-rejT, the cytotoxicities of DRrejT and LMP2-rejT were compared by ^{51}Cr release assay. At an E : T ratio of 10:1, DRrejT killed HLA-A*2402$^+$ LCL (autologous LCL) with 82.0±20.1% specific lysis, whereas LMP2-

rejT showed lower levels of killing, with 62.0±4.5% specific lysis (p=0.1679, unpaired Student's *t* test). LMP2-rejT, which require HLA-restricted antigen recognition, could not kill HLA-A*2402$^-$ LCL (0.5 ± 1.6%, E : T ratio 10:1, DRrejT; p=0.0022, LMP2-rejT; p<0.0001, unpaired Student's *t* test) (Figure 2F).

To examine the LMP1-CAR cytotoxicity of DRrejT, HLA-A*2402$^-$ LCL cells were cocultured with DRrejT. On day 7 of coculture at E : T ratio 5:1, DRrejT could eliminate HLA-A*2402$^-$ LCL through CAR recognition (CD19$^+$ and CD3$^-$, 11.5% day 0 to 1.4% day 7), whilst control rejT not specifically responsive to EBV antigen could not eliminate HLA-A*2402$^-$ LCL, which thereupon proliferated (CD19$^+$ and CD3$^-$, 11.0% day 0 to 50.7% day 7) (Figure 2G left). The absolute cell number of HLA-A*2402$^-$ LCL cocultured with DRrejT decreased from 86,565 ± 7,941 (Day 0) to 36,148 ± 4,282 (Day 7), whereas that of HLA-A*2402$^-$ LCL cocultured with control rejT rapidly increased from 92,450 ± 8,091 (Day 0) to 370,255 ± 14,009 (Day 7) (Figure 2G, right). Furthermore, we examined the LMP1-CAR cytotoxicity of DRrejT using the HLA-A*2402$^-$ ENKL cell line SNK-6. At an E : T ratio of 10:1, DRrejT killed SNK-6 with 53.3±18.0% specific lysis, whereas DRrejT did not kill EBV$^-$ tumor cells (control target), with 8.6±4.8% specific lysis (p=0.0107, unpaired Student's *t* test) (Figure 2H). As killing of LMP2-rejT via TCR against HLA-A*2402$^+$ ENKL was also strong, although additive killing via LMP1-CAR was shown, its extent was not statistically significant (Figure 2F). However, using HLA mismatched LCL and ENKL cell lines permitted clear demonstration of reliable cytotoxicity of DRrejT via LMP1-CAR (Figure 2G and Figure 2H).

Furthermore, to prove the anti-tumor effect of DRrejT using primary ENKL cells, we assayed the cytotoxicity of DRrejT against HLA-A*2402$^+$ patient ENKL cells (42% of tumor-infiltrated bone marrow) by ^{51}Cr release. Strong killing of DRrejT was successfully demonstrated against

HLA-A*2402$^+$ primary ENKL cells. At an E : T ratio of 10:1, DRrejT killed ENKL primary cells with 60.7±8.6% specific lysis, but did not kill control target (p=0.0008, unpaired Student's *t* test) (Figure 2I).

These data suggested that DRrejT exhibited an additional killing effect, owing to CAR, beyond that of LMP2-rejT and also possessed cytotoxicity not only against HLA-mismatched LMP1$^+$ tumor cells but even against primary ENKL cells.

All DRrejT treated mice survived for more than 100 days

To assess the additive killing effect of DRrejT over LMP2-rejT against LMP1$^+$ EBV-associated lymphoma cells *in vivo*, we also intraperitoneally engrafted NOG mice with 1x10^5 GFP/FFLuc-NK-YS cells. Four days after tumor injection, mice were divided into a control group and 2 treatment groups. No treatment was given in the control group (n=5). The treatment groups (n=5 each) were treated with LMP2-rejT on day 0, day 7, and day 14 (5x10^6 cells / dose, 3 doses) and DRrejT on day 0, day 7, and day 14 (5x10^6 cells / dose, 3 doses). Tumor signals in both DRrejT and LMP2-rejT treated mice were suppressed, but the tumor-suppressive effect was clearly stronger in the DRrejT treatment group than in the LMP2-rejT treatment group (Figure 3A). Furthermore, DRrejT and LMP2-rejT conferred a significant survival advantage over the no treatment group（p=0.0033, p=0.03, respectively; log-rank test）, and all mice treated with DRrejT survived more than 110d after the first rejT dose (Figure 3B). Mouse peripheral blood was stained with anti-human CD3 antibodies and HLA-A*2402/LMP2$_{131\text{-}139}$ tetramer, with analysis by flow cytometry, 101d after the first rejT dose. Human CD3$^+$ lymphocytes were detected in peripheral blood of both DRrejT treated and LMP2-rejT treated mice, but were proportionally more abundant in DRrejT treated mice (35.8%) than in LMP2-rejT treated mice

(3.05%). In addition, tetramer$^+$/CD3$^+$ lymphocytes were detected in peripheral blood of DRrejT treated mice, as well as, in smaller numbers, in that of LMP2-rejT treated mice (Figure 3C).

In conclusion, DRrejT strongly suppressed ENKL, markedly prolonged the survival of treated mice, and persisted long-term in mouse peripheral blood.

DRrejT could eliminate re-inoculated tumor cells

To evaluate whether DRrejT were actually present *in vivo* and were still effective, we inoculated a second dose of 1x10^5 ENKL cells into mice surviving the previous experiment more than 110d after the first rejT dose; 3 mice received a second dose of ENKL in the DRrejT group and 2 received a second dose of ENKL in the LMP2-rejT group. Both DRrejT and LMP2-rejT gradually eliminated re-inoculated ENKL cells over 60d without any additional treatment（Figure 4A）. Flow cytometry was also used to detect DRrejT or LMP2-rejT in peripheral blood of long-term surviving mice before and after re-inoculation of ENKL cells（Figure 4B）. Although LMP2 tetramer$^+$/CD3$^+$ rejT were not detected in peripheral blood of LMP2-rejT treated mice before ENKL re-inoculation, they reappeared 4d after ENKL re-inoculation（Figure 4B, upper）. In contrast, LMP2 tetramer$^+$/CD3$^+$ DRrejT were clearly detectable in peripheral blood of treated mice even before re-inoculation, and their population increased after re-inoculation（Figure 4B, lower）. In addition, to examine whether rejT were existing as memory T cells *in vivo*, CD45RA and CD62L expression in mouse peripheral blood was analyzed. The major population was shifted from effector memory phenotype (CD45RA$^-$ CD62L$^-$) towards central memory phenotype (CD45RA$^-$ CD62L$^+$) in peripheral blood of mice treated with either LMP2-rejT or DRrejT (Figure 4C).

Collectively, these data demonstrated that DRrejT persisted long-term as young memory T cells *in vivo* and successfully eliminated re-inoculated ENKL cells.

iC9-safeguard system induced apoptosis in DRrejT

To confirm effective function of the iC9 safeguard system in this therapy model, DRrejT into which iC9 had been introduced and LMP2-rejT were plated and treated with a chemical inducer of dimerization (CID; AP1903 or its functionally identical analog AP20187) 24h later. In the presence of CID, dimerized iC9 directly activates caspase-3, triggering apoptosis in transduced cells [17, 24, 25, 28-30]. Annexin-V phycoerythrin (Annexin V) binding and 7-amino-actinomycin D (7-AAD) uptake were examined 48h after CID addition. CID induced apoptosis in iC9-introduced DRrejT (with CID, 91.19%; without CID, 4.0%). In contrast, CID administration did not significantly increase apoptosis in LMP2-rejT (with CID, 16.8%; without CID, 13.7%). The absolute number of apoptotic DRrejT increased to 598,907 ± 63,833 with CID from 19,780 ± 2,997 without CID ($p<0.0001$, two-way ANOVA), whereas it did not change in LMP2-rejT with CID 72,271 ± 6,152 and without CID 60,776 ± 2,689, $p=0.9064$, two-way ANOVA) (Figure 4D).

Thus, the iC9 system can induce apoptosis in iC9-introduced DRrejT and provides an effective safeguard for this therapy in case of cytokine-release syndrome, acute graft-versus-host disease, or other unexpected adverse effects.

DRrejT targeting CD19 and LMP2 antigens robustly suppressed the proliferation of LCL

To examine whether DRrejT with another combination of target antigens also efficiently suppress tumor proliferation, we generated DRrejT directed against CD19 antigen via CAR and against LMP2 antigen via native TCR. LMP2-rejT was directly transduced with retroviral CD19-CAR in this experiment. We also generated retroviral CD19-CAR transduced human papilloma virus (HPV)-specific rejT (CD19-CAR/HPV-rejT) as a control targeted against a single antigen. CAR transgene expression in both CD19-CAR/HPVrejT and DRrejT was ~70-80%. After GFP/FFLuc-labeled HLA-A*2402^{+} LCL (CD19^{+} and LMP2^{+}) were intraperitoneally engrafted into NOG mice on day -3, LMP2-rejT, CD19-CART, or DRrejT were injected into the mice in the treatment groups on day 0, day 7, and day 14. The tumor signals in mice without treatment aggressively increased with time (Figure 5A). On the other hand, LMP2-rejT clearly suppressed tumor proliferation. Compared with mice without treatment, LMP2-rejT and CD19-CAR/HPV-rejT produced a significant reduction in tumor burden on day18 ($p=0.003$ and 0.0101; one-way ANOVA) (Figure 5B). DRrejT further suppressed proliferation of EBV^{+} LCL (Figure 5A) and robustly reduced tumor signal compared with untreated mice ($p<0.0001$; one-way ANOVA), even with CD19-CAR/HPV-rejT treated mice ($p=0.0349$; one-way ANOVA) on day 18 (Figure 5B).

Furthermore, LMP2-rejT, CD19-CAR/HPV-rejT and DRrejT clearly prolonged survival of mice compared to mice without treatment ($p=0.0047$, $p=0.0253$, and 0.0016 by log-rank test, respectively). DRrejT conferred upon mice a survival advantage superior to that of mice treated with LMP2-rejT ($p=0.0154$; log-rank test). The tumor suppressive effect of DRrejT was better, with longer survival, than that found in mice treated with CD19-CAR/HPV-rejT ($p=0.0031$; log-rank test) (Figure 5C). To confirm whether DRrejT and LMP2-rejT could efficiently proliferate *in vivo*, LMP2 tetramer^{+} and human CD3^{+} positivity in mouse peripheral blood was examined. A

small LMP2 tetramer^{+} / CD3^{+} population was detected in peripheral blood of a LMP2-rejT treated mouse (0.41%), CD19-CAR/HPV-rejT treated mice (0.89%), with a larger one in peripheral blood of a DRrejT treated mouse (2.42%) (Figure 5D). On day 48, CD19-CAR copy number per microgram genomic DNA in peripheral blood was 1066462.4 ± 37349.9 in a mouse treated with DRrejT, showing that DRrejT efficiently expanded and persisted *in vivo*. On the other hand, CD19-CAR copy number was 123135.1 ±17245.5 in a mouse treated with CD19-CAR/HPV-rejT and significantly lower than that of DRrejT treated mouse ($p<0.0001$ by one-way ANOVA). CD19-CAR transduced T cells with 76% CAR transgene expression 4 days after CD19-CAR transduction were used as positive control (992987.7 ± 24039.7) (Figure 5E).

DRrejT targeting CD19 and LMP2 antigens thus also robustly suppressed tumor growth of LCL, conferred a survival advantage, and efficiently expanded *in vivo* with high CD19-CAR transgene expression, permitting similar conclusions in two *in vivo* models.

Discussion

Because tumors exhibit a number of escape mechanisms, early and multi-faceted intervention is required for efficient anti-tumor therapy. EBV-associated lymphoma cells express LMP1 and LMP2 in many cases [20, 31, 32], good targets for CAR on the cell surface and for TCR in association with HLA class I antigens. To target both LMP1 and LMP2, we generated iPSC-derived dual-antigen receptor bearing CTL, *viz.*, DRrejT.

In this study, CAR transgene expression in peripheral blood-derived LMP1-CART was ~25% (Figure 1C), whereas that of iPSC-derived DRrejT was 100% (Figure 1F). Because iPSC are an excellent platform for gene transduction [17, 18, 22], transgene expression of lentiviral LMP1-CAR carrying *Ubc* promoter into T-iPSC was ~90% after the first transduction (data not shown). As

the *Ubc* promoter provides stable expression of the transgene [17], CAR transgene expression was still high after differentiation into DRrejT (Figure 1F). The robust cytotoxicity shown against EBV-associated lymphoma was consistent with the high transgene expression in DRrejT (Figure 2A); DRrejT exhibit sustained tumor suppression *in vivo* (Figure 2B). A clear survival advantage over peripheral-blood LMP1-CART was also shown (Figure 2C). Furthermore, DRrejT targeting CD19 and LMP2 antigens conferred survival in tumor-inoculated mice longer than that conferred by single antigen targeted T cells, CD19-CAR transduced HPV-rejT, and LMP2-rejT. To obtain a better result, DRrejT might be generated from lentiviral CD19-CAR-iPSC, resulting in stable CAR transgene expression of 100%.

Furthermore, as DRrejT are the descendants of LMP1-CAR-transduced T-iPSC established from LMP2-CTL clones, LMP2 antigen specificity of DRrejT was also nearly 100% (Figure 1F). Based on LMP2-specific cytotoxicity, killing of LMP1-CAR contributed to the additive cytotoxicity of DRrejT against EBV-associated lymphomas *in vitro* (Figure 2F) and *in vivo* (Figure 3A). As most adults are infected with EBV and are seropositive, LMP2-rejT are theoretically stimulated effectively by engagement of native TCR and LMP2-antigen presenting tumor cells [33]. Therefore, we think that to use LMP2-rejT as a vehicle for CAR is reasonable in DRrejT therapy.

We further demonstrated that DRrejT gradually eliminated even re-inoculated ENKL without additional treatment (Figure 4A). Effector and central memory T cells were detected in peripheral blood of treated mice. The population shifted from effector to central memory phenotype after tumor re-inoculation (Figure 4C), suggesting that rejuvenated central memory-phenotype DRrejT persist strongly and prevent tumor relapse *in vivo*. Exclusive sampling of peripheral blood in the xenograft experiments does not consider homing of DRrejT to secondary

lymphoid organs; however, DRrejT may home to spleen or lymph nodes and persist long-term, causing elimination of ENKL[20].

Tandem CART cells engage 2 antigens on glioblastomas simultaneously by inducing heterodimers, which promotes additive T cell activation when both antigens are encountered concurrently [34]. However, many tumors do not express 2 suitable antigens on the cell surface. Although antigen recognition by DRrejT proceeds differently from that by tandem CART cells, the powerful anti-tumor effect of DRrejT might be attributable to its dual-antigen recognition ability, with not only LMP1 or CD19 recognition by CAR but also LMP2 recognition by native TCR. If targeting both tumor antigens simultaneously, accelerated tumor elimination becomes possible and the emergence of resistance to therapy can be avoided [35]. Using several cell lines permitted confirmation of the efficient function of DRrejT. In addition, results of killing assays in an ENKL patient bone-marrow sample infiltrated by tumor further emphasized the likely clinical applicability of this work.

The important advantage of iPSC-derived DRrejT therapy is that once T-iPSC are established from CTL clones and CAR is transduced into established T-iPSC, one can unlimitedly generate therapeutic DRrejT from T-iPSC. Repeated administration of large numbers of DRrejT to patients, with rapid and powerful killing by DRrejT, would prevent antigen escape relapse. If we generate from healthy donors several iPSC lines originating from different HLA-restricted LMP2-CTL and edit HLA class I to avoid rejection by host immune cells, DRrejT therapy will be suitable for a great number of patients and true “off-the-shelf” therapy will be feasible.

When rejT are generated from patient peripheral blood T cells, GVHD is infrequent. However, triggering severe toxicity by CART cell expansion, modifying T cell trafficking, or effector activity remains a concern [23]. To make adoptive DRrejT therapy safer, we equipped DRrejT with

an iC9 safety system. Indeed, administration of the dimerizer CID efficiently induced apoptosis in DRrejT that included this system (Figures 4D). In clinical translation, one must pay attention to the oncogenic risk of iPSC caused by lentiviral transduction. CAR-iPSC can be cloned, analyzed for copy number, and selected for a minimum number of oncogenic mutations. Should an undesired event happen in spite of these validation processes, the iC9 safety system will be useful: Its introduction into iPSC-derived DRrejT therapy mitigates possible toxicity and tumorigenic risk of CART therapy[17]. Our work thus serves as proof-of-concept that novel DRrejT therapy can overcome the drawbacks of conventional CTL and CART therapy.

Methods

Cell lines

Dr. Junjiroh Tsuchiyama, Okayama University Medical School, Okayama, Japan kindly provided the HLA-A*2402^{+} ENKL cell line NK-YS [20, 36]. NK-YS cells were grown in Iscove's modified Dulbecco's medium (IMDM) (Gibco, Carlsbad, CA) supplemented with 10% fetal bovine serum (FBS) (Gibco), 100U/ml penicillin, 100µg/ml streptomycin, 2mM L-glutamine (Gibco), and 100IU/ml interleukin (IL)-2 (Miltenyi Biotec, Bergisch Gladbach, Germany) [37]. Dr. Norio Shimizu, Tokyo Medical and Dental University, Tokyo, Japan, kindly provided the HLA-A*2402^{-} ENKL cell line SNK-6[20, 38]. SNK-6 cells were grown in NS-A2 medium (Nissui, Tokyo, Japan) supplemented with 10% FBS (Gibco) and 100IU/ml IL-2 (Miltenyi Biotec). EBV^{+}LCL were derived from PBMC in our laboratory using EBV isolated from B95-8 cell lines in the presence of cyclosporin A. Donor B lymphocytes were infected with EBV and transformed into LCL [39-42]. EBV^{+}LCL were grown in Roswell Park Memorial Institute 1640 medium (Gibco) supplemented with 10% FBS (Gibco), 100U/ml penicillin, 100µg/ml

streptomycin, and 2mM L-glutamine (Gibco). Cells from the EBV^- osteosarcoma cell line, HOS (ATCC, Manassas, VA), were grown in IMDM (Gibco) supplemented with 10% FBS (Gibco), 100U/ml penicillin, 100µg/ml streptomycin, and 2mM L-glutamine (Gibco).

Clinical sample

Bone marrow infiltrated by ENKL primary cells from a patient diagnosed with ENKL (2014) at Juntendo University School of Medicine, Department of Hematology, were used for ^{51}Cr release assay. ENKL was diagnosed on histopathologic study of a skin biopsy specimen (READ, Koutoubiken, Tokyo, Japan) according to World Health Organization classification guidelines. Bone marrow infiltration (42%) was also diagnosed. Bone marrow mononuclear cells, including ENKL cells, were separated and frozen-stored. Cell viability in a thawed aliquot was > 80%. Mononuclear cells, not further sorted or selected, were used for ^{51}Cr release assay. Use of material and of clinical information was approved by the Research Ethics Committee for the Faculty of Medicine, Juntendo University, and was in accordance with the Declaration of Helsinki.

Immunohistochemical staining

Immunoperoxidase studies were performed on formalin-fixed paraffin sections with a horseradish peroxidase conjugated polymer method. Anti-LMP1 mouse monoclonal antibody (CS.1-4; 1:100 dilution; M0897, Dako, Glostrup, Denmark) was used for immunostaining [43]. Anti-LMP1 antibody was applied after antigen retrieval following microwave oven heating treatment.

In situ *hybridization*

For *in situ* hybridization to detect EBV RNA, the tissue was hybridized with oligo-probe EBER-1 (AGACACCGTCCTCACCACCCGGGACTTGTA) and sense probe (negative control), labelled with digoxigenin [44]. After dewaxing, dehydration, and protein K digestion, sections were hybridized overnight in a solution of 50% formamide containing 5ng digoxigenin-labelled probes. After washing, detection was accomplished using an avidin-alkaline phosphatase conjugate, with diaminobenzidine as the chromogen.

Vector construction and virus production

DNA sequences of the variable regions of light chain (VL) and heavy chain (VH) of human anti-LMP1 are reported [45]. Synthesized 2A-VL-Linker-VH-hinge (GenScript, Piscataway, NJ) was amplified by polymerase chain reaction (PCR) and fused to the Psi I-Pflm I site of the template SFG-iC9-2A-14G2a (GD2)-CD28-OX40z by replacing GD2-CD28-OX40z with LMP1-CD28-OX40z. To generate a lentiviral CAR vector construct, the Leader-LMP1-CD28-OX40z was amplified by PCR and then fused into the Xba I-Xho I site of the lentiviral Cs-Ubc-iC9-F2A-mCherry construct by replacing mCherry with LMP1-CD28-OX40. After Cs-Ubc-iC9-F2A-LMP1-CD28-OX40z was generated, lentiviral vectors pseudotyped with the vesicular stomatitis virus G glycoprotein were produced in cultured 293T cells as described [17, 46]. Virus supernatants were collected 48h-72h later. The pan-caspase inhibitor qVD-Oph (R&D Systems, Minneapolis, MN) (20μM) was added to the medium to protect 293T cells during lentivirus production [17]. CD19-4-1BBz amplified by PCR was fused into the EcoR I-Xho I site of the MSCV-IRES-GFP-construct (Addgene, Watertown, MA). After MSCV-CD19-4-1BBz-IRES-GFP was generated, 293T cells were transfected with the retroviral construct Peg-Pam-e, encoding gag-pol, and RDF,

encoding the RD114 envelope, using GeneJuice transfection reagent (Sigma-Aldrich, St. Louis, MO). Supernatants were collected 48-72h later as described [28]. The vector encoding *GFP/FFLuc* is described [47].

Peripheral blood-derived CART cell generation

PBMC of healthy donors were activated by anti-CD3 antibody and anti-CD28 antibody (both Biolegend) in the presence of IL-2 (100U/ml). Three days later, activated T cells were seeded onto 24-well plates coated with RetroNectin (Takara Bio, Shiga, Japan) and LMP1-CAR lentiviral supernatants or CD19-CAR retroviral supernatants were added to each well. CART cells were cultured in NS-A2 (Nissui) with 10ng/ml each of IL-7 and IL-15 (Miltenyi Biotec).

EBV-specific CTL generation

PBMC were isolated from an HLA-A*2402 positive healthy donor (the institutional regulation boards for human ethics at Juntendo University School of Medicine and at the Institute of Medical Science, University of Tokyo, approved the experimental protocol). They were cocultured with autologous dendritic cells (DC) presenting the LMP2-derived peptide PYLFWLAAI (Mimotopes, Victoria, Australia) or TYGPVFMSL (MBL, Nagoya, Japan) in the presence of IL-4 (400IU/ml) and IL-7 (10ng/ml; both Miltenyi Biotec) [48, 49]. On day 9 of culture, T cells were restimulated with peptide-pulsed DC. On day 16, CTL were stained with HLA-A*2402/LMP2$_{131\text{-}139}$ tetramer or A*2402/LMP2$_{419\text{-}427}$ tetramer (MBL) and tetramer-reactive CTL were cloned by limiting dilution to obtain LMP2-specific CTL clones [16, 17, 20].

T-iPSC establishment from EBV-specific CTL clones

An EBV-antigen-directed LMP2-CTL clone (PYLFWLAAI) was transduced with Sendai virus vectors encoding the Yamanaka 4 factors OCT3/4, SOX2, KLF4, and c-MYC and SV40 large T antigen. Another LMP2-CTL clone (TYGPVFMSL) was transduced with Sendai virus vector encoding the Yamanaka 4 factors, NANOG, and LIN28 [21]. Transduced cells were transferred onto plates coated with iMatrix-511 (Nippi, Tokyo, Japan) and cultured in NS-A2. Growth medium was gradually replaced with StemFit AK03N (Ajinomoto Healthy Supply, Tokyo, Japan). After ~14d, iPSC colonies were picked up into new culture wells and passaged in CTS Essential 8 medium (Thermo Fisher Scientific, Waltham, MA) several times until cell numbers sufficed for studies [20].

LMP1-CAR transduction into T-iPSC

T-iPSC established from LMP2-CTL clone (PYLFWLAAI) ($1x10^5$ cells) were transduced with LMP1-CAR lentiviral vector on vitronectin (Thermo Fisher Scientific) coated plates (multiplicity of infection 20) and cultured in CTS Essential 8 medium (Thermo Fisher Scientific). On day 9, transduced iPSC were stained with biotinylated protein L (Thermo Fisher Scientific) followed by APC streptavidin (BD Biosciences, San Jose, CA). LMP1-CAR^+ iPSC were sorted several times by flow cytometry.

Redifferentiation of T-iPSC into DRrejT

Small clumps of LMP1-CAR-T-iPSC were plated on C3H10T1/2 feeder cells in IMDM supplemented with γ-irradiated 15% FBS (HyClone, GE Healthcare UK, Little Chalfont, UK) and a cocktail of 10mg/ml insulin, 5.5mg/ml transferrin, 5ng/ml sodium selenite, 2mM L-glutamine (Thermo Fisher Scientific), 0.45mM a-monothioglycerol (Sigma-Aldrich), and

50mg/ml ascorbic acid (Takeda Pharmaceutical Company, Tokyo, Japan) in the presence of 20ng/ml vascular endothelial growth factor (Miltenyi Biotech). On day 14 of coculture, sac-like structures that contained hematopoietic progenitor cells were extracted and transferred onto Delta-like ligands 1- and 4-expressing C3H10T1/2 feeder cells in α-MEM (Thermo Fisher Scientific) with FBS (HyClone), in the presence of 20ng/ml human stem cell factor, 10ng/ml human Fms-related tyrosine kinase 3 ligand (both Miltenyi Biotec), and 10ng/ml IL-7. On day 28 of coculture, T-lineage cells were harvested, stimulated by irradiated PBMC in NS-A2 in the presence of phytohemagglutinin (Sigma-Aldrich), 5mg/ml, and of IL-7 and IL-15 (Miltenyi Biotech), 10ng/ml each. C3H10T1/2, DL1/4-expressing C3H10T1/2 feeder cell lines and γ-irradiated FBS (HyClone) have already been validated are compatible with Good Manufacturing Practice standard for clinical use. Master cell bank stocks were made.

LMP2 specificity and LMP1-CAR transgene expression were confirmed by staining with HLA-A*2402/LMP2$_{131\text{-}139}$ tetramer and biotinylated Protein L respectively (GenScript) followed by streptavidin-APC (BD Biosciences).

Generation of DRrejT targeting CD19 and LMP2 antigens

T-iPSC established from LMP2-CTL clone (TYGPVFMSL) were differentiated into LMP2-rejT as described. LMP2 specificity was confirmed by staining with HLA-A*2402/LMP2$_{419\text{-}427}$ tetramer. Next, LMP2-rejT were transduced with MSCV-CD19-4-1BBz-IRES-GFP and GFP$^+$ cells were sorted by flow cytometry. As a single antigen-targeted control, HPV16 E6-specific rejT[21] were transduced with MSCV-CD19-4-1BBz-IRES-GFP; GFP$^+$ cells among CD19-CAR/HPV-rejT were also sorted by flow cytometry. CD19-CAR transgene expression of DRrejT and CD19-CAR/HPV-rejT was confirmed by GFP positivity on flow cytometric analysis.

Flow cytometric analyses

Samples were processed using FACS Aria II, LSRFortessa, and FACS Calibur cytometers (BD Biosciences). The results were analyzed using FlowJo software 10.5.3 (Tree Star, Ashland, OR). After cells were incubated with the appropriate concentration of fluorescence-conjugated monoclonal antibody cocktail for 30 minutes at 4℃, they were washed with phosphate-buffered saline. Propidium iodide was added to exclude dead cells. Chromophore-conjugated monoclonal antibodies directed against surface antigens were used; they included APC mouse anti-human CD3 antibody, APC mouse anti-human CD4 antibody, APC mouse anti-human CD19 antibody, APC mouse anti-human CD279 (PD-1), APC cyanin 7 mouse anti-human CD3 antibody, fluorescein isothiocyanate (FITC) mouse anti-human CD19 antibody, phycoerythrin (PE) mouse anti-human CD4 antibody, PE mouse anti-human CD56 antibody, PE mouse anti-human CD62L antibody, Pacific Blue mouse anti-human CD8, Pacific Blue mouse anti-human CD45RA antibody (all Biolegend), and FITC mouse anti-human CD3 antibody (BD Biosciences). To detect CAR expression, CAR transduced cells were stained with biotinylated recombinant Protein L (GenScript), followed by APC-conjugated streptavidin (BD Biosciences). PE conjugated HLA-A*2402/LMP2$_{131\text{-}139}$ tetramer, A*2402/LMP2$_{419\text{-}427}$ tetramer, or A*2402/HPV16 E6$_{419\text{-}427}$ tetramer (MBL) was used to detect antigen specific TCR.

Coculture experiments

For serial killing experiments with PBMC-derived LMP1-CART, expanded LMP1-CART and non-transduced activated T cells (used as effector control cells) were cocultured with LCL at the E : T ratio of 1 : 1 ($1x10^5$: $1x10^5$ cells) in NS-A2 with IL-7 and IL-15, 10ng/ml each. Cultures

were collected at days 0, 5, and 7 of coculture and stained with anti-CD3 and -CD19 antibodies. Percentages of $CD3^+$ $CD19^-$ T cells and $CD19^+$ $CD3^-$ tumor cells were evaluated by flow cytometry. For serial killing experiments with iPSC-derived DRrejT, DRrejT and control rejT not specific to EBV antigen also were cocultured with HLA-A*2402$^+$ *GFP/FFluc* ENKL or HLA-A*2402$^-$(mismatched) LCL at the E : T ratio of 5 : 1 ($5x10^5$: $1x10^5$ cells) in NS-A2 with IL-7 and IL-15, 10 ng/ml each. Although CD3 is useful when separating tumor cells from rejT, to separate these populations using CD3 and GFP/CD19 expression in coculture assays gave clearer results. Cultures were collected at days 0, 5, and 7 of coculture and stained with anti-CD3 (*GFP/FFluc* NK-YS) or anti-CD3 and -CD19 antibodies (LCL). Percentages of $CD3^+$ T cells and $CD3^-$ tumor cells were evaluated by flow cytometric analysis. To count absolute cell numbers by flow cytometry, CountBright Absolute Counting Beads (Thermo Fisher Scientific) were added (20μl) [50]. Absolute numbers of tumor cells were calculated according to the manufacturer's protocol.

^{51}Cr release assay

Cytotoxic specificities of DRrejT, LMP1-CART, LMP1-CAR/HPV-rejT and LMP2-rejT were analyzed in a standard chromium-51 release assay at different E : T ratios [51]. Target cells were labeled with ^{51}Cr and cocultured with T cells for 20h. After incubation, 50 μl of supernatant was transferred from each well to LumaPlate-96 wells (PerkinElmer, Waltham, MA) and dried overnight. Released Cr was quantitated using a TopCount microplate scintillation counter (PerkinElmer), with % specific lysis = ([experimental Cr release] – [spontaneous Cr release] / [maximal Cr release] – [spontaneous Cr release]) x 100.

In vivo *experiments*

All *in vivo* studies were approved by the Animal Research Committees of The Institute of Medical Science, The University of Tokyo, and of Juntendo University School of Medicine.

NK-YS and EBV-infected LCL transduced with γ-retroviral vector encoding *GFP/FFluc* were sorted for GFP expression by flow cytometry. Six-week-old female NOD/Shi-scid, IL-2RγKO Jic (NOG) mice (In-Vivo Science, Tokyo, Japan) were intraperitoneally engrafted with *GFP/FFluc* NK-YS ($1x10^5$ cells). Mice were divided into 3 groups, with 2 treatment groups and one no treatment group. Four days after tumor inoculation, mice in treatment groups were intraperitoneally injected with DRrejT or peripheral blood-derived LMP1-CART to compare the anti-tumor effect of these therapeutic T cells (Figure 2B) and with DRrejT or LMP2-rejT, to compare the anti-tumor effect of these therapeutic rejT (Figure 3A) ($5x10^6$ cells, once a week, 3 doses) followed by intraperitoneal injection of recombinant IL2, 1000U/mouse, once a week. Six-week-old female NOG mice (In-Vivo Science) were intraperitoneally engrafted with *GFP/FFluc* LCL ($0.8x10^5$ cells). Mice were divided into 4 groups, with 3 treatment groups and one no-treatment group. Three days after tumor inoculation, mice in the 3 treatment groups were intraperitoneally injected with LMP2-rejT, CD19-CAR transduced HPV-rejT, or DRrejT to compare the anti-tumor effect of these therapeutic T cells (Figure 5A) ($4x10^6$ cells, once a week, 3 doses) followed by intraperitoneal injection of recombinant IL2, 1000U/mouse, 5 times a week. Tumor-bearing mice were randomized to the different treatment groups. No blinding method was used. We repeated in vivo experiments twice to confirm the reproducibility of the results. Tumor burden was monitored by the Xenogen IVIS imaging system (Xenogen, Alameda, CA) and Caliper IVIS imaging system (Caliper Life Sciences, Mountain View, CA). Firefly D-luciferin substrate (OZ Biosciences, Marseille, France) was intraperitoneally injected into mice

15min before imaging. Living Image software version 2.50 (Xenogen) and Living Image software version 4.7.2 (PerkinElmer) were used for luminescence analyses. The intensity of signal was measured as total photon/s/cm^2/steradian (p/s/cm^2/sr) as described [17, 20].

Quantitative real-time PCR

Genomic DNA was isolated from samples of mouse whole blood and cultured CD19-CART cells using a QIAamp DNA Blood Mini Kit (Qiagen, Hilden, Germany). CD19-CAR vector copy number was quantified using the StepOnePlus real-time PCR system (Applied Biosystems, Carlsbad, CA). Primer and probes for the CD19-CAR transgene and GAPDH were custom-ordered (Applied Biosystems) as described [52]. Individual PCR reactions were normalized against GAPDH levels. Copies transgene / microgram DNA were calculated according to the formula: copies calculated from CD19 standard curve/input DNA (ng) x correction factor (ng detected/ng input) x 1000 ng, as described [53].

Measurement of apoptosis

On the day after 2x10^5 DRrejT or LMP2-rejT were plated into 24-well plates, CID/AP20187 (Clontech, Mountain View, CA), 80nmol/l, was added to the wells. The cells were stained 24h later with Annexin-V and 7AAD for 15 min according to the manufacturer's instructions (BD Biosciences). Annexin-V/7-AAD$^+$ cells were quantitated by FACS Aria II flow cytometry using FlowJo software. To count absolute numbers of apoptotic cells by flow cytometry, CountBright Absolute Counting Beads were added. Acquisition was halted at 2000 beads [50].

Statistical analysis

All data are presented as mean ± SD or SEM as stated in the figure legends. Results were analyzed by ANOVA or unpaired Student's *t* test as stated in the text. Comparison of survival curves was done using Kaplan-Meier analysis with log-rank testing. All statistical analyses were performed using Excel (Microsoft, Redmond, WA) and Prism (GraphPad Software, San Diego, CA) programs. Values of $p<0.05$ were considered significant.

Acknowledgments

We thank A.S. Knisely for critical reading of the manuscript; Risa Matsuoka for technical help with cell culture; Nozomi Asano for technical help in making the LMP1-CAR vector; and Azusa Fujita, Yumiko Ishii, and Tamami Sakanishi for FACS operation. Malcolm K Brenner provided retroviral iC9-GD2-CAR plasmid. Gianpietro Dotti and Nobuhiro Nishio provided retroviral FFluc-GFP plasmid. We also thank Motoo Watanabe and Hajime Yasuda for helpful discussions. We thank the members of the Laboratory of Radioisotope Research, Research Support Center, Juntendo University Graduate School of Medicine for technical assistance. This work was carried out in part at the Intractable Disease Research Center, Juntendo University Graduate School of Medicine. The institutional regulation boards for human ethics at Juntendo University School of Medicine and at the Institute of Medical Science, University of Tokyo, approved the experimental protocol. The project was supported by JSPS KAKENHI (grants 16K09842 and 19K07781) and a Grant for Cross-disciplinary Collaboration, Juntendo University (30-52).

Competing interests

HN is a co-founder of and an advisor to Century Therapeutics.

Author contributions

M.A. planned and directed the study and wrote the manuscript. S.H. performed the experiments and wrote the manuscript. J.A. performed ^{51}Cr assays and provided scientific discussions. M.I., S.Y., and K.O. helped in animal experiments. T.T. performed ^{51}Cr assays and helped in animal experiments. C.I. provided retroviral CD19-CAR plasmid. T.Y., Y.N., C.S., and C.I. helped in making CAR constructs. M.O and M.N. provided SeV vectors. Y.O., K. N., and K.O. helped in immunohistochemical staining. H.N. wrote the manuscript, and provided scientific discussions. N.K. provided scientific discussions.

Figure Legends

Fig. 1. **Generation and validation of LMP1-CART cells.**

(**A**) LMP1 expression and EBV-encoded small RNA (EBER) *in situ* hybridization of EBV$^+$ cell lines and EBV$^-$ cell line as negative control. (**B**) Schematic of the lentiviral iC9-CAR vector containing Ubc promoter. CAR contains a scFv derived from heavy (VH) and light chain (VL) variable regions of an anti-LMP1 antibody. Transmembrane (TM): CD28. The vector contains the suicide gene iC9, cleavable 2A-like sequence. (**C**) Flow cytometric analysis of expression of LMP1-CAR in PMBC-derived LMP1-CART cells detected by protein L which binds to scFv of CAR, followed by streptavidin-APC staining and determination of APC signal. The data represent at least 5 independent experiments using 4 different donors. (**D**) PBMC-derived LMP1-CART cells and lymphoblastoid cell lines (LCL) were cocultured (ratio 1:1). Cultures were collected, stained with anti-CD3 and -CD19 antibodies, and analyzed by flow cytometry on days 0, 5, and 7. The plots represent 3 independent experiments. Cells were counted using counting

beads on flow cytometry. Graph summarizes the results of total cell number of LCL. Error bars represent ± SEM. **** $p<0.0001$ by two-way ANOVA. (**E**) Schematic illustrations of generation of LMP2-rejT and DRrejT. T-iPSC established from LMP2-specific CTL clones were differentiated into LMP2-rejT. T-iPSC established from LMP2-specific CTL clones were transduced with lentiviral LMP1-CAR vector and LMP1-CAR-T-iPSC were differentiated into DRrejT. (**F**) Flow cytometric analysis of LMP1-CAR transgene expression (left), CD4 and CD8 expression (center), and LMP2-antigen specificity detected by PE-conjugated HLA-A*2402/$LMP2_{131-139}$ tetramer (right) in DRrejT. (**G**) Programmed cell death 1 (PD-1) expression in LMP1-CART and DRrejT detected by flow cytometry. Error bars represent ± SD. ** $p<0.01$ by unpaired Student's *t* test. The plots represent 4 independent experiments.

Fig. 2. DRrejT exhibit cytotoxicity against EBV-associated lymphoma superior to LMP1-CART and LMP2-rejT.

(**A**) *In vitro* ^{51}Cr release assay of iPSC-derived DRrejT and PBMC-derived LMP1-CART cells (effectors) against HLA-A*2402^{+} ENKL and HLA-A*2402^{-} LCL (targets). Error bars represent ± SD. Data represent 3 independent triplicate experiments. (**B**) NOG mice were intraperitoneally inoculated with HLA-matched ENKL cells expressing firefly luciferase and treated either with PBMC-derived LMP1-CART (n=7) or iPSC-derived DRrejT(n=8). No treatment indicates that mice were injected with ENKL cells but not treated with T cells (n=5). LMP1-CART or DRrejT were injected intraperitoneally once a week (3 doses). Images of all mice from each group of 2 independent experiments are shown. (**C**) Kaplan-Meier curve representing percentage survival of experimental groups: no treatment, LMP1-CART, or DRrejT. ***$P<0.001$ and ****$P<0.0001$ by log-rank test. (**D**) *In vitro* ^{51}Cr release assay of iPSC-derived DRrejT and LMP1-CAR transduced

HPV-rejT (LMP1-CAR/HPV-rejT) (effectors) against HLA-A*2402^{+} LCL and LMP1^{-} tumor (targets). Error bars represent ± SD. Data represent 3 independent triplicate experiments. (**E**) iPSC-derived DRrejT and control rejT were cocultured with HLA-A*2402^{+} GFP/FFluc ENKL (ratio 5:1). Cultures were collected, stained with anti-CD3 antibody, and analyzed by flow cytometry on days 0, 5 and 7. The plots represent 3 independent experiments. Cells were counted using counting beads on flow cytometry. Graph summarizes the results of total cell number of NK-YS. Error bars represent ± SEM. **** p<0.0001 by two-way ANOVA. (**F**) *In vitro* ^{51}Cr release assay of iPSC-derived DRrejT and LMP2-rejT (effectors) against HLA-A*2402^{+} LCL and HLA-A*2402^{-} LCL (targets). Error bars represent ± SD. Data represent 3 independent triplicate experiments. (**G**) iPSC-derived DRrejT and control rejT were cocultured with HLA-A*2402^{-} LCL (ratio 5:1). Cultures were collected, stained with anti-CD3 and -CD19 antibodies, and analyzed by flow cytometry on days 0, 5 and 7. The plots represent 3 independent experiments. Cells were counted using counting beads on flow cytometry. Graph summarizes the results of total cell number of LCL. Error bars represent ± SEM. **** p<0.0001 by two-way ANOVA. E : T ratio, effector: target ratio. (**H**) *In vitro* ^{51}Cr release assay of DRrejT (effector) against HLA-A*2402^{-} ENKL and EBV^{-} tumor (targets). Error bars represent ± SD. (**I**) *In vitro* ^{51}Cr release assay of DRrejT (effector) against HLA-A*2402^{+} ENKL primary cells and EBV^{-} tumor (targets). Error bars represent ± SD. *<p<0.1, **P<0.01 and ***P<0.001 by unpaired Student's *t* test.

Fig. 3. DRrejT display additive anti-ENKL activity over LMP2-rejT *in vivo*.

(**A**) Bioluminescence imaging of mice treated with LMP2-rejT or DRrejT. ENKL-bearing mice were divided into 3 groups that received no treatment (n=5), LMP2-rejT (n=5), or DRrejT (n=5).

No treatment indicates that mice were injected with ENKL cells but not treated with T cells. LMP2-rejT or DRrejT ($5x10^6$ cells) were injected intraperitoneally once a week (3 doses). Data represent at least 2 independent experiments. (**B**) Kaplan-Meier curve representing percentage survival of the experimental groups: no treatment, LMP2-rejT, or DRrejT. **P<0.01 and *P<0.05 by log-rank test. ns, not significant. (**C**) Flow cytometric analysis of $tetramer^+/CD3^+$ population from peripheral blood of LMP2-rejT or DRrejT treated mice. Plots represent 2 independent experiments.

Fig. 4. DRrejT eliminate re-inoculated ENKL.

(**A**) LMP2-rejT treated or DRrejT treated ENKL-inoculated mice were re-inoculated with ENKL cells. Bioluminescence imaging of re-inoculated mice: LMP2-rejT treated mice (n=2) or DRrejT treated mice (n=3). ENKL ($1x10^5$ cells) were injected intraperitoneally into survivors of a previous experiment, without additional rejT. (**B**) Flow cytometric analysis of $tetramer^+/CD3^+$ population from peripheral blood of LMP2-rejT or DRrejT treated ENKL-re-inoculated mice. The plots represent 2 independent experiments. (**C**) Flow cytometric analysis of memory phenotype (CD45RA and CD62L population) from peripheral blood of LMP2-rejT or DRrejT treated ENKL-re-inoculated mice. The plots represent 2 independent experiments. (**D**) LMP2-rejT (no iC9) and DRrejT (with iC9) were treated with CID (80nM) and apoptosis was measured 24h later by flow cytometry for annexin V/7-AAD positivity. Data represent 3 independent triplicate experiments. Cells were counted using counting beads on flow cytometry. Graph summarizes the results of total apoptotic cell number. Error bars represent ± SD. ****p<0.0001 by two-way ANOVA. ns, not significant.

Fig. 5. DRrejT robustly suppressed LCL.

(**A**) Bioluminescence imaging of mice treated with LMP2-rejT, CD19-CAR transduced HPV-rejT (CD19-CAR/HPV-rejT) or DRrejT. EBV^{+}LCL-bearing mice were divided into 4 groups that received no treatment (n=5), LMP2-rejT (n=4), CD19-CAR/HPV-rejT (n=4), or DRrejT (n=6). No treatment indicates mice that were injected with LCL cells but not treated with T cells. LMP2-rejT, CD19-CAR/HPV-rejT or DRrejT ($4x10^6$ cells) were injected intraperitoneally once a week (3 doses). Images of all mice from each group of 2 independent experiments are shown. (**B**) Quantification of tumor burden on day 18 is represented. ****p<0.0001, **P<0.01 and *P<0.05 by one-way ANOVA. (**C**) Kaplan-Meier curve representing percentage survival of the experimental groups: no treatment, LMP2-rejT, CD19-CAR/HPV-rejT or DRrejT. **P<0.01 and *P<0.05 by log-rank test. (**D**) Flow cytometric analyses of peripheral blood of LMP2-rejT(day 42), CD19-CAR/HPV-rejT(day 23), or DRrejT(day 42) treated LCL-inoculated mice. The plots represent 3 independent experiments. (**E**) CD19-CAR persisted in peripheral blood of mice treated with CD19-CAR/HPV-rejT on day 23 or DRrejT on day 48. Copy number of CD19-CAR transduced T cells, positive control. Error bars represent ± SD. ****p<0.0001 by one-way ANOVA. Data represent 3 independent triplicate experiments.

References

1. June, CH, and Sadelain, M (2018). Chimeric antigen receptor therapy. *The New England journal of medicine* **379**: 64-73.
2. Lim, WA, and June, CH (2017). The principles of engineering immune cells to treat cancer. *Cell* **168**: 724-740.
3. Rafiq, S, Hackett, CS, and Brentjens, RJ (2020). Engineering strategies to overcome the current roadblocks in CAR T cell therapy. *Nature reviews Clinical oncology* **17**: 147-167.
4. Jackson, HJ, Rafiq, S, and Brentjens, RJ (2016). Driving CAR T-cells forward. *Nature reviews Clinical oncology* **13**: 370-383.

5. Brudno, JN, and Kochenderfer, JN (2018). Chimeric antigen receptor T-cell therapies for lymphoma. *Nature reviews Clinical oncology* **15**: 31-46.
6. Grupp, SA, Kalos, M, Barrett, D, Aplenc, R, Porter, DL, Rheingold, SR, *et al.* (2013). Chimeric antigen receptor-modified T cells for acute lymphoid leukemia. *The New England journal of medicine* **368**: 1509-1518.
7. Lee, DW, Kochenderfer, JN, Stetler-Stevenson, M, Cui, YK, Delbrook, C, Feldman, SA, *et al.* (2015). T cells expressing CD19 chimeric antigen receptors for acute lymphoblastic leukaemia in children and young adults: a phase 1 dose-escalation trial. *Lancet* **385**: 517-528.
8. Park, JH, Riviere, I, Gonen, M, Wang, X, Senechal, B, Curran, KJ, *et al.* (2018). Long-term follow-up of CD19 CAR Therapy in acute lymphoblastic leukemia. *The New England journal of medicine* **378**: 449-459.
9. Turtle, CJ, Hanafi, LA, Berger, C, Gooley, TA, Cherian, S, Hudecek, M, *et al.* (2016). CD19 CAR-T cells of defined CD4+:CD8+ composition in adult B cell ALL patients. *The Journal of clinical investigation* **126**: 2123-2138.
10. Shah, NN, and Fry, TJ (2019). Mechanisms of resistance to CAR T cell therapy. *Nature reviews Clinical oncology* **16**: 372-385.
11. Orlando, EJ, Han, X, Tribouley, C, Wood, PA, Leary, RJ, Riester, M, *et al.* (2018). Genetic mechanisms of target antigen loss in CAR19 therapy of acute lymphoblastic leukemia. *Nature medicine* **24**: 1504-1506.
12. Majzner, RG, and Mackall, CL (2018). Tumor antigen escape from CAR T-cell therapy. *Cancer Discovery* **8**: 1219-1226.
13. Wherry, EJ (2011). T cell exhaustion. *Nature immunology* **12**: 492-499.
14. Maude, SL, Laetsch, TW, Buechner, J, Rives, S, Boyer, M, Bittencourt, H, *et al.* (2018). Tisagenlecleucel in children and young adults with B-cell lymphoblastic leukemia. *The New England journal of medicine* **378**: 439-448.
15. Schuster, SJ, Svoboda, J, Chong, EA, Nasta, SD, Mato, AR, Anak, O, *et al.* (2017). Chimeric antigen receptor T cells in refractory B-cell lymphomas. *The New England journal of medicine* **377**: 2545-2554.
16. Nishimura, T, Kaneko, S, Kawana-Tachikawa, A, Tajima, Y, Goto, H, Zhu, D, *et al.* (2013). Generation of rejuvenated antigen-specific T cells by reprogramming to pluripotency and redifferentiation. *Cell stem cell* **12**: 114-126.
17. Ando, M, Nishimura, T, Yamazaki, S, Yamaguchi, T, Kawana-Tachikawa, A, Hayama, T, *et al.* (2015). A safeguard system for induced pluripotent stem cell-derived rejuvenated T cell therapy. *Stem cell reports* **5**: 597-608.

18. Ando, M, and Nakauchi, H (2017). 'Off-the-shelf' immunotherapy with iPSC-derived rejuvenated cytotoxic T lymphocytes. *Experimental hematology* **47**: 2-12.
19. Vizcardo, R, Masuda, K, Yamada, D, Ikawa, T, Shimizu, K, Fujii, S, *et al.* (2013). Regeneration of human tumor antigen-specific T cells from iPSCs derived from mature CD8(+) T cells. *Cell stem cell* **12**: 31-36.
20. Ando, M, Ando, J, Yamazaki, S, Ishii, M, Sakiyama, Y, Harada, S, *et al.* (2020). Long-term eradication of extranodal natural killer/T-cell lymphoma, nasal type, by induced pluripotent stem cell-derived Epstein-Barr virus-specific rejuvenated T cells in vivo. *Haematologica* **105**: 796-807.
21. Honda, T, Ando, M, Ando, J, Ishii, M, Sakiyama, Y, Ohara, K, *et al.* (2020). Sustainable tumor suppressive effect of iPSC-derived rejuvenated T cells targeting cervical cancers. *Molecular Therapy* **28**: 2394-2405.
22. Themeli, M, Riviere, I, and Sadelain, M (2015). New cell sources for T cell engineering and adoptive immunotherapy. *Cell stem cell* **16**: 357-366.
23. Heczey, A, Louis, CU, Savoldo, B, Dakhova, O, Durett, A, Grilley, B, *et al.* (2017). CAR T cells administered in combination with lymphodepletion and PD-1 Inhibition to patients with neuroblastoma. *Molecular therapy* **25**: 2214-2224.
24. Straathof, KC, Pulè, MA, Yotnda, P, Dotti, G, Vanin, EF, Brenner, MK, *et al.* (2005). An inducible caspase 9 safety switch for T-cell therapy. *Blood* **105**: 4247-4254.
25. Di Stasi, A, Tey, SK, Dotti, G, Fujita, Y, Kennedy-Nasser, A, Martinez, C, *et al.* (2011). Inducible apoptosis as a safety switch for adoptive cell therapy. *The New England journal of medicine* **365**: 1673-1683.
26. Zheng, Z, Chinnasamy, N, and Morgan, RA (2012). Protein L: a novel reagent for the detection of chimeric antigen receptor (CAR) expression by flow cytometry. *Journal of translational medicine* **10**: 29. (http://www.translational-medicine.com/content/10/1/29)
27. Heslop, HE (2005). Biology and treatment of Epstein-Barr virus-associated non-Hodgkin lymphomas. *Hematology American Society of Hematology Education Program*: 260-266.
28. Ando, M, Hoyos, V, Yagyu, S, Tao, W, Ramos, CA, Dotti, G, *et al.* (2014). Bortezomib sensitizes non-small cell lung cancer to mesenchymal stromal cell-delivered inducible caspase-9-mediated cytotoxicity. *Cancer gene therapy* **21**: 472-482.
29. Itakura, G, Kawabata, S, Ando, M, Nishiyama, Y, Sugai, K, Ozaki, M, *et al.* (2017). Fail-safe system against potential tumorigenicity after transplantation of iPSC derivatives. *Stem cell reports* **8**: 673-684.

30. Hoyos, V, Del Bufalo, F, Yagyu, S, Ando, M, Dotti, G, Suzuki, M, *et al.* (2015). Mesenchymal stromal cells for linked delivery of oncolytic and apoptotic adenoviruses to non-small-cell lung cancers. *Molecular therapy* **23**: 1497-1506.
31. Chiang, AK, Tao, Q, Srivastava, G, and Ho, FC (1996). Nasal NK- and T-cell lymphomas share the same type of Epstein-Barr virus latency as nasopharyngeal carcinoma and Hodgkin's disease. *International journal of cancer* **68**: 285-290.
32. Fox, CP, Haigh, TA, Taylor, GS, Long, HM, Lee, SP, Shannon-Lowe, C, *et al.* (2010). A novel latent membrane 2 transcript expressed in Epstein-Barr virus-positive NK- and T-cell lymphoproliferative disease encodes a target for cellular immunotherapy. *Blood* **116**: 3695-3704.
33. Pulè, MA, Savoldo, B, Myers, GD, Rossig, C, Russell, HV, Dotti, G, *et al.* (2008). Virus-specific T cells engineered to coexpress tumor-specific receptors: persistence and antitumor activity in individuals with neuroblastoma. *Nature medicine* **14**: 1264-1270.
34. Hegde, M, Mukherjee, M, Grada, Z, Pignata, A, Landi, D, Navai, SA, *et al.* (2016). Tandem CAR T cells targeting HER2 and IL13Ralpha2 mitigate tumor antigen escape. *The Journal of clinical investigation* **126**: 3036-3052.
35. Fry, TJ, Shah, NN, Orentas, RJ, Stetler-Stevenson, M, Yuan, CM, Ramakrishna, S, *et al.* (2018). CD22-targeted CAR T cells induce remission in B-ALL that is naive or resistant to CD19-targeted CAR immunotherapy. *Nature medicine* **24**: 20-28.
36. Tsuchiyama, J, Yoshino, T, Mori, M, Kondoh, E, Oka, T, Akagi, T, *et al.* (1998). Characterization of a novel human natural killer-cell line (NK-YS) established from natural killer cell lymphoma/leukemia associated with Epstein-Barr virus infection. *Blood* **92**: 1374-1383.
37. Ando, M, Sugimoto, K, Kitoh, T, Sasaki, M, Mukai, K, Ando, J, *et al.* (2005). Selective apoptosis of natural killer-cell tumours by l-asparaginase. *British journal of haematology* **130**: 860-868.
38. Nagata, H, Konno, A, Kimura, N, Zhang, Y, Kimura, M, Demachi, A, *et al.* (2001). Characterization of novel natural killer (NK)-cell and gammadelta T-cell lines established from primary lesions of nasal T/NK-cell lymphomas associated with the Epstein-Barr virus. *Blood* **97**: 708-713.
39. Anderson, MA, and Gusella, JF (1984). Use of cyclosporin A in establishing Epstein-Barr virus-transformed human lymphoblastoid cell lines. *In vitro* **20**: 856-858.
40. Miller, G, and Lipman, M (1973). Comparison of the yield of infectious virus from clones of human and simian lymphoblastoid lines transformed by Epstein-Barr virus. *The Journal of experimental medicine* **138**: 1398-1412.
41. Smith, CA, Ng, CY, Heslop, HE, Holladay, MS, Richardson, S, Turner, EV, *et al.* (1995). Production of genetically modified Epstein-Barr virus-specific cytotoxic T cells for adoptive

transfer to patients at high risk of EBV-associated lymphoproliferative disease. *Journal of hematotherapy* **4**: 73-79.

42. Ando, J, Ngo, MC, Ando, M, Leen, A, and Rooney, CM (2020). Identification of protective T-cell antigens for smallpox vaccines. *Cytotherapy*.

43. Oyama, T, Ichimura, K, Suzuki, R, Suzumiya, J, Ohshima, K, Yatabe, Y, *et al.* (2003). Senile EBV+ B-cell lymphoproliferative disorders: a clinicopathologic study of 22 patients. *The American journal of surgical pathology* **27**: 16-26.

44. Ohshima, K, Suzumiya, J, Kanda, M, Haraoka, S, Kawasaki, C, Shimazaki, K, *et al.* (1999). Genotypic and phenotypic alterations in Epstein-Barr virus-associated lymphoma. *Histopathology* **35**: 539-550.

45. Chen, R, Zhang, D, Mao, Y, Zhu, J, Ming, H, Wen, J, *et al.* (2012). A human Fab-based immunoconjugate specific for the LMP1 extracellular domain inhibits nasopharyngeal carcinoma growth in vitro and in vivo. *Molecular cancer therapeutics* **11**: 594-603.

46. Yamaguchi, T, Hamanaka, S, Kamiya, A, Okabe, M, Kawarai, M, Wakiyama, Y, *et al.* (2012). Development of an all-in-one inducible lentiviral vector for gene specific analysis of reprogramming. *PloS one* **7**: e41007.

47. Quintarelli, C, Vera, JF, Savoldo, B, Giordano Attianese, GM, Pulè, M, Foster, AE, *et al.* (2007). Co-expression of cytokine and suicide genes to enhance the activity and safety of tumor-specific cytotoxic T lymphocytes. *Blood* **110**: 2793-2802.

48. Gerdemann, U, Keirnan, JM, Katari, UL, Yanagisawa, R, Christin, AS, Huye, LE, *et al.* (2012). Rapidly generated multivirus-specific cytotoxic T lymphocytes for the prophylaxis and treatment of viral infections. *Molecular therapy* **20**: 1622-1632.

49. Rooney, CM, Leen, AM, Vera, JF, and Heslop, HE (2014). T lymphocytes targeting native receptors. *Immunological reviews* **257**: 39-55.50.Torres Chavez, A, McKenna, MK, Canestrari, E, Dann, CT, Ramos, CA, Lulla, P, *et al.* (2019). Expanding CAR T cells in human platelet lysate renders T cells with in vivo longevity. *Journal for immunotherapy of cancer* **7**: 330. https://doi.org/10.1186/s40425-019-0804-9

51. Rooney, CM, Smith, CA, Ng, CY, Loftin, SK, Sixbey, JW, Gan, Y, *et al.* (1998). Infusion of cytotoxic T cells for the prevention and treatment of Epstein-Barr virus-induced lymphoma in allogeneic transplant recipients. *Blood* **92**: 1549-1555.

52. Milone, MC, Fish, JD, Carpenito, C, Carroll, RG, Binder, GK, Teachey, D, *et al.* (2009). Chimeric receptors containing CD137 signal transduction domains mediate enhanced survival of T cells and increased antileukemic efficacy in vivo. *Molecular therapy* **17**: 1453-1464.

53. Kalos, M, Levine, BL, Porter, DL, Katz, S, Grupp, SA, Bagg, A, *et al.* (2011). T cells with chimeric antigen receptors have potent antitumor effects and can establish memory in patients with advanced leukemia. *Science translational medicine* **3**: 95ra73.

Figure 1

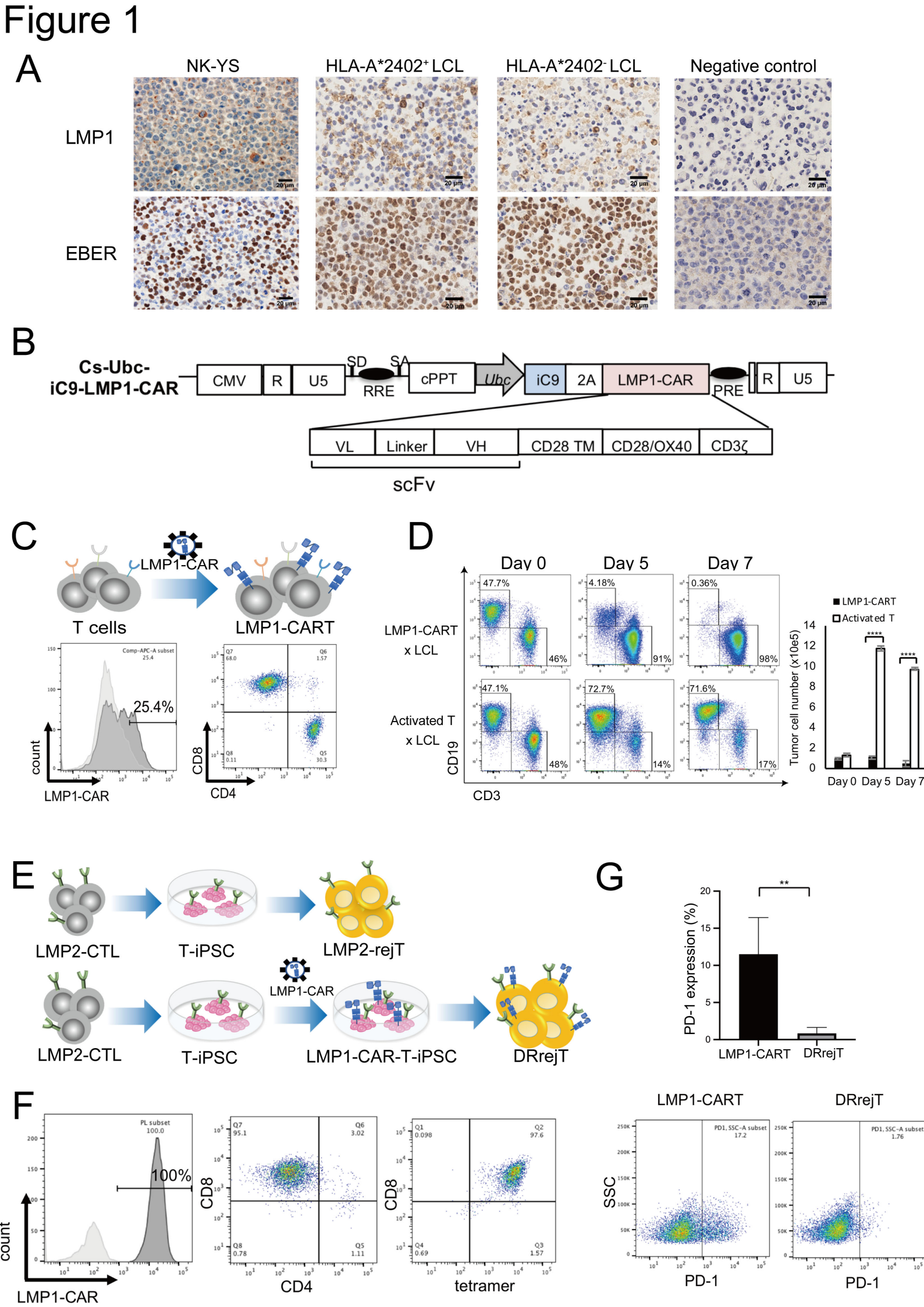
A
NK-YS
HLA-A*2402+ LCL
HLA-A*2402- LCL
Negative control
LMP1
EBER
20 μm
B
Cs-Ubc-iC9-LMP1-CAR
CMV
R
U5
SD
SA
RRE
cPPT
Ubc
iC9
2A
LMP1-CAR
PRE
R
U5
VL
Linker
VH
CD28 TM
CD28/OX40
CD3ζ
scFv
C
LMP1-CAR
T cells
LMP1-CART
25.4%
count
LMP1-CAR
CD8
CD4
D
Day 0
Day 5
Day 7
LMP1-CART x LCL
Activated T x LCL
47.7%
46%
4.18%
91%
0.36%
98%
47.1%
48%
72.7%
14%
71.6%
17%
CD19
CD3
LMP1-CART
Activated T
Tumor cell number (x10e5)
****
****
Day 0
Day 5
Day 7
E
LMP2-CTL
T-iPSC
LMP2-rejT
LMP1-CAR
LMP2-CTL
T-iPSC
LMP1-CAR-T-iPSC
DRrejT
G
**
PD-1 expression (%)
LMP1-CART
DRrejT
F
100%
count
LMP1-CAR
CD8
CD4
tetramer
LMP1-CART
DRrejT
SSC
PD-1
PD-1

Figure 2

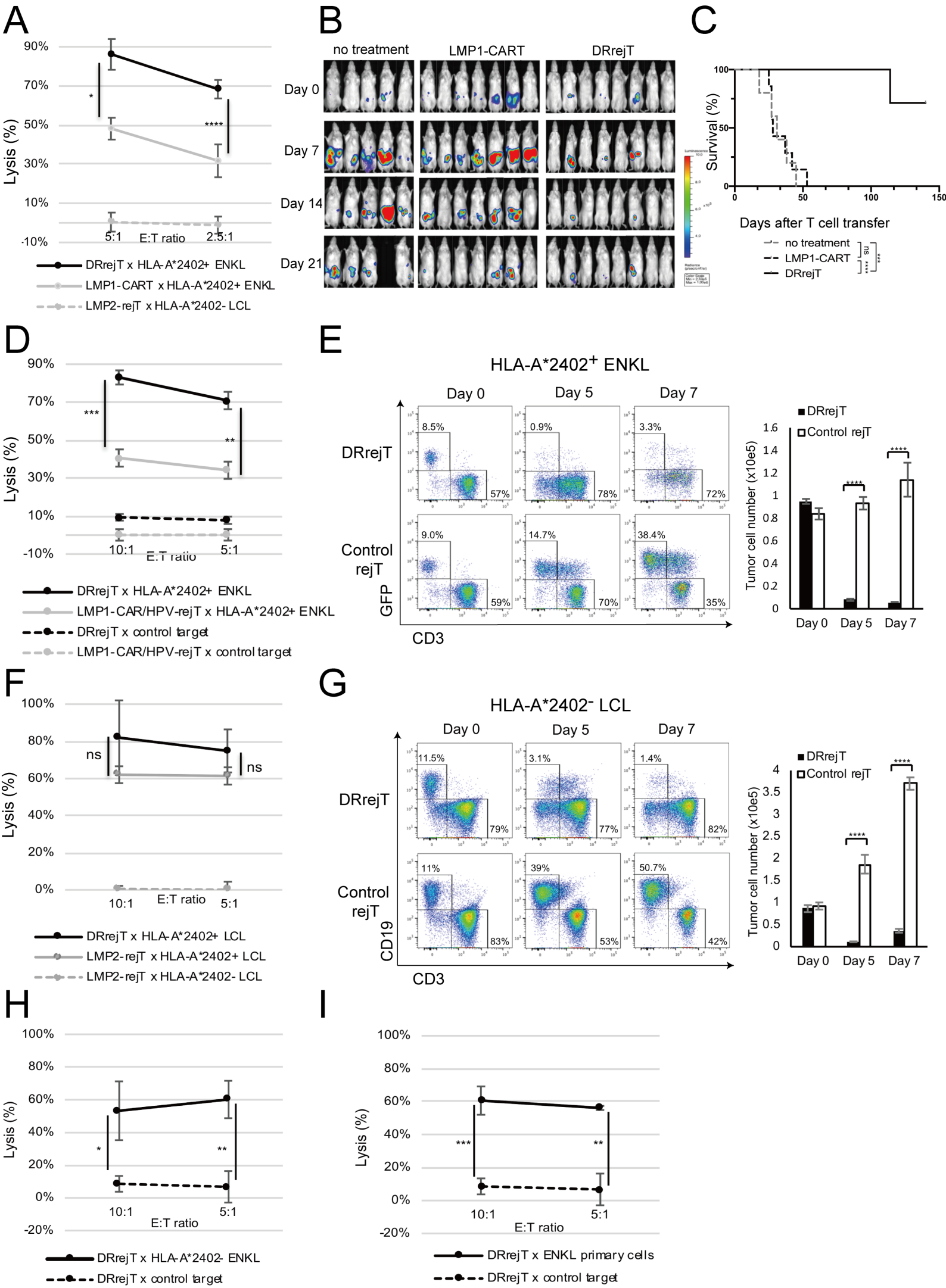
A
90%
70%
50%
30%
10%
-10%
Lysis (%)
*
****
5:1
E:T ratio
2.5:1
DRrejT x HLA-A*2402+ ENKL
LMP1-CART x HLA-A*2402+ ENKL
LMP2-rejT x HLA-A*2402- LCL
B
no treatment
LMP1-CART
DRrejT
Day 0
Day 7
Day 14
Day 21
C
100
50
0
Survival (%)
0
50
100
150
Days after T cell transfer
no treatment
LMP1-CART
DRrejT
ns
***
****
D
90%
70%
50%
30%
10%
-10%
Lysis (%)
***
**
10:1
E:T ratio
5:1
DRrejT x HLA-A*2402+ ENKL
LMP1-CAR/HPV-rejT x HLA-A*2402+ ENKL
DRrejT x control target
LMP1-CAR/HPV-rejT x control target
E
HLA-A*2402+ ENKL
Day 0
Day 5
Day 7
DRrejT
Control rejT
8.5%
57%
0.9%
78%
3.3%
72%
9.0%
59%
14.7%
70%
38.4%
35%
GFP
CD3
DRrejT
Control rejT
Tumor cell number (x10e5)
1.6
1.4
1.2
1
0.8
0.6
0.4
0.2
0
****
****
Day 0
Day 5
Day 7
F
100%
80%
60%
40%
20%
0%
Lysis (%)
ns
ns
10:1
E:T ratio
5:1
DRrejT x HLA-A*2402+ LCL
LMP2-rejT x HLA-A*2402+ LCL
LMP2-rejT x HLA-A*2402- LCL
G
HLA-A*2402- LCL
Day 0
Day 5
Day 7
DRrejT
Control rejT
11.5%
79%
3.1%
77%
1.4%
82%
11%
83%
39%
53%
50.7%
42%
CD19
CD3
DRrejT
Control rejT
Tumor cell number (x10e5)
4
3.5
3
2.5
2
1.5
1
0.5
0
****
****
Day 0
Day 5
Day 7
H
100%
80%
60%
40%
20%
0%
-20%
Lysis (%)
*
**
10:1
E:T ratio
5:1
DRrejT x HLA-A*2402- ENKL
DRrejT x control target
I
100%
80%
60%
40%
20%
0%
-20%
Lysis (%)
***
**
10:1
E:T ratio
5:1
DRrejT x ENKL primary cells
DRrejT x control target

igure 3

A

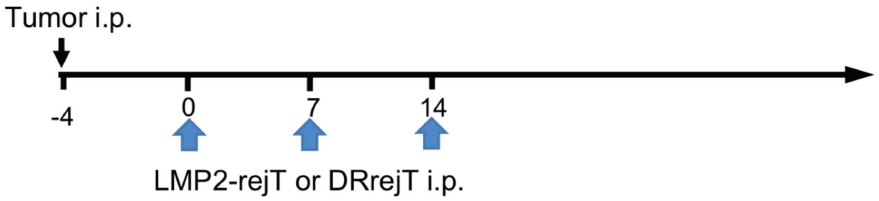
Tumor i.p.
-4
0
7
14
LMP2-rejT or DRrejT i.p.

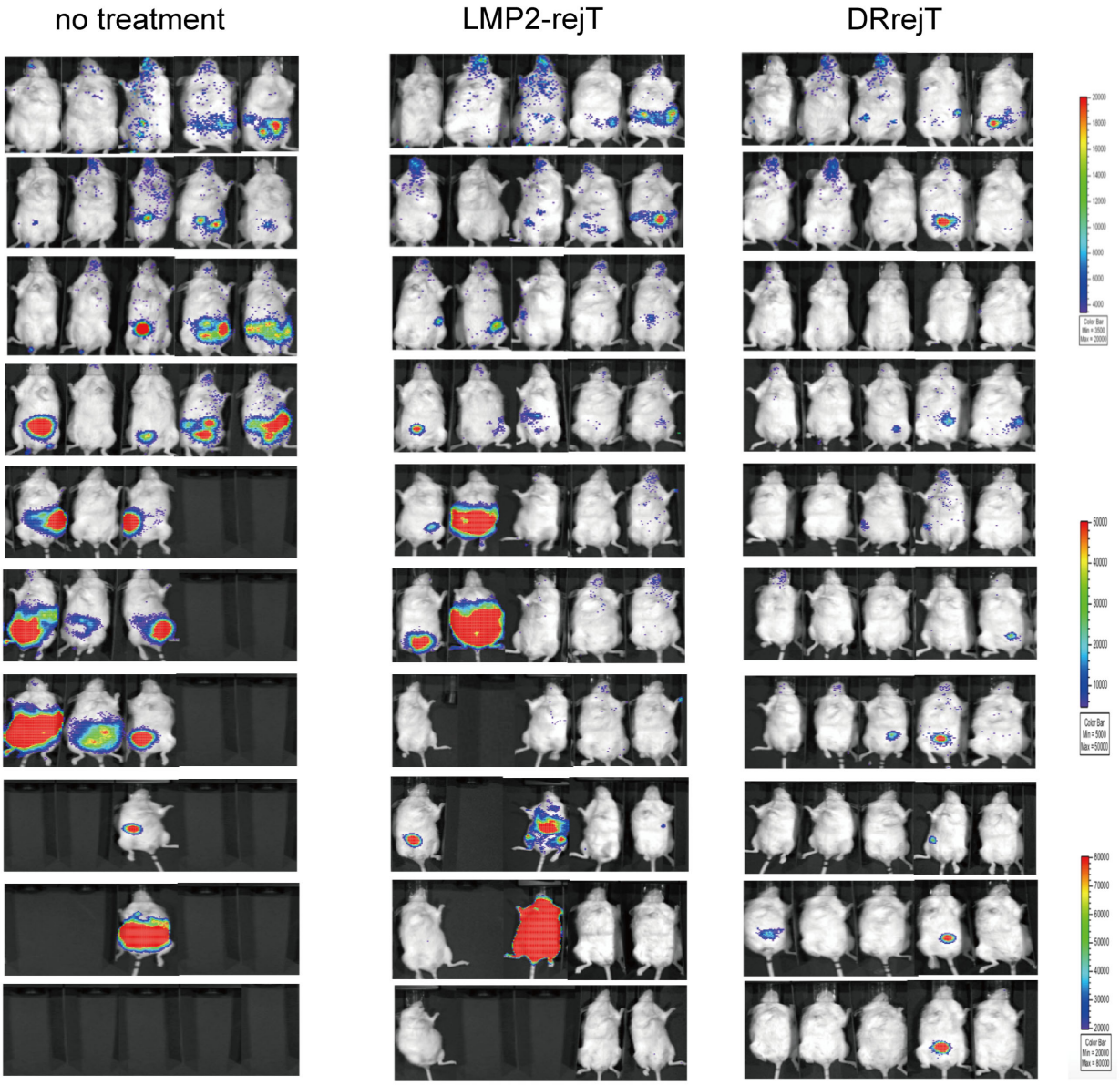
no treatment
LMP2-rejT
DRrejT
Day 0
Day 7
Day 14
Day 21
Day 40
Day 53
Day 60
Day 80
Day 101
Day 112

B

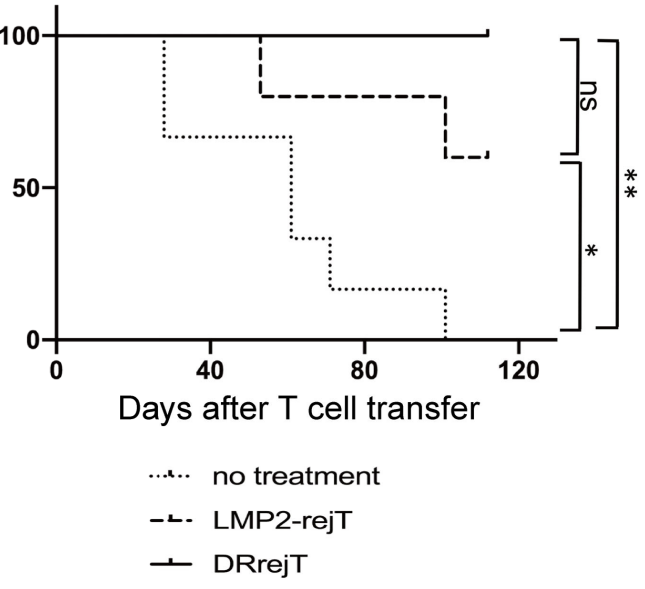
100
50
0
0
40
80
120
Days after T cell transfer
ns
*
**
no treatment
LMP2-rejT
DRrejT

C

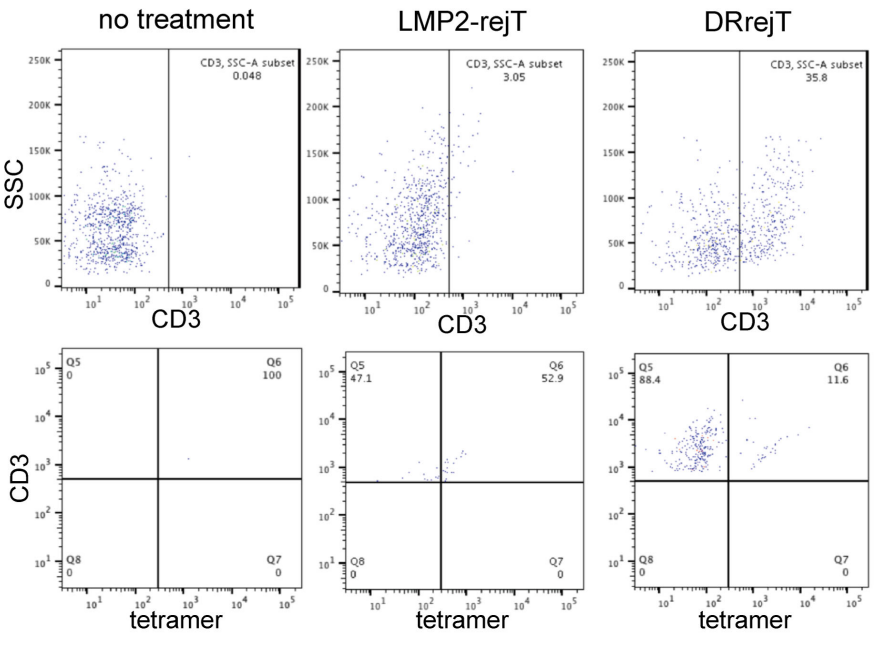
no treatment
LMP2-rejT
DRrejT
CD3, SSC-A subset
0.048
3.05
35.8
SSC
CD3
Q5
Q6
Q8
Q7
100
47.1
52.9
88.4
11.6
tetramer

Figure 4

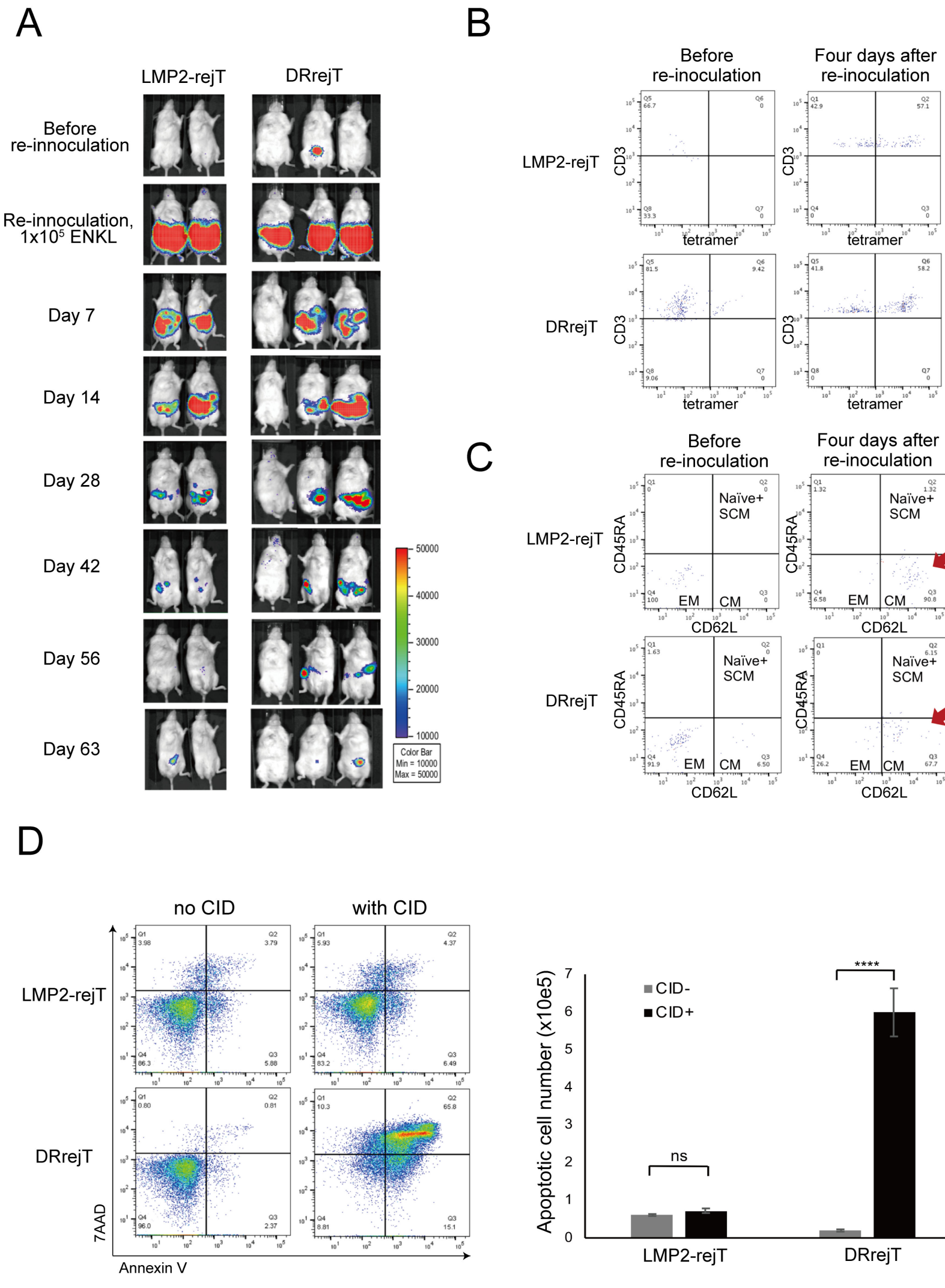
A
LMP2-rejT
DRrejT
Before re-innoculation
Re-innoculation, 1x10^5 ENKL
Day 7
Day 14
Day 28
Day 42
Day 56
Day 63
50000
40000
30000
20000
10000
Color Bar
Min = 10000
Max = 50000
B
Before re-inoculation
Four days after re-inoculation
LMP2-rejT
DRrejT
CD3
tetramer
C
Before re-inoculation
Four days after re-inoculation
LMP2-rejT
DRrejT
CD45RA
CD62L
Naïve+ SCM
EM
CM
D
no CID
with CID
LMP2-rejT
DRrejT
7AAD
Annexin V
Apoptotic cell number (x10e5)
CID-
CID+
ns
****
LMP2-rejT
DRrejT

Figure 5

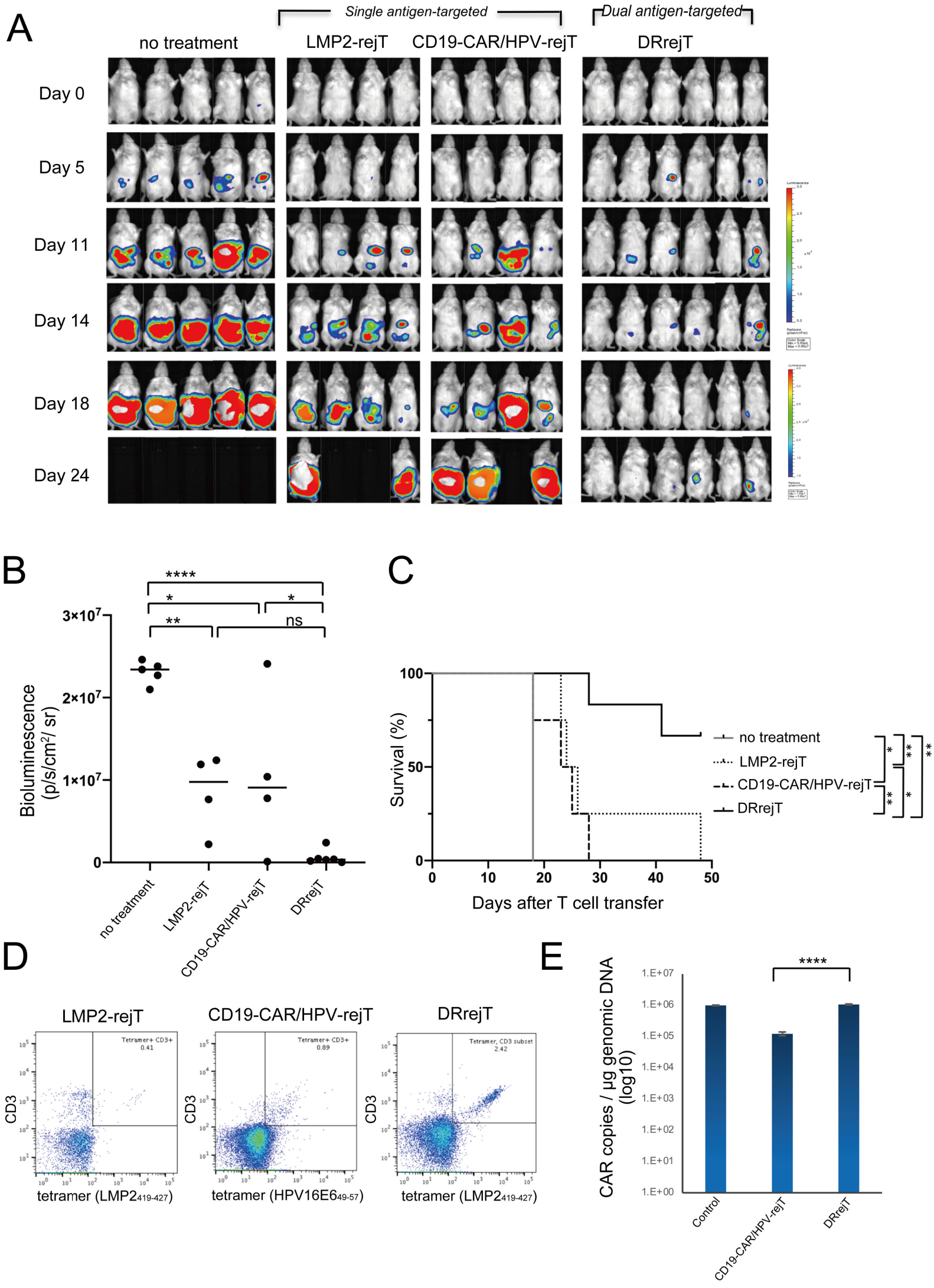
A
Single antigen-targeted
Dual antigen-targeted
no treatment
LMP2-rejT
CD19-CAR/HPV-rejT
DRrejT
Day 0
Day 5
Day 11
Day 14
Day 18
Day 24
B
Bioluminescence (p/s/cm²/ sr)
3×10⁷
2×10⁷
1×10⁷
0
****
*
*
**
ns
no treatment
LMP2-rejT
CD19-CAR/HPV-rejT
DRrejT
C
Survival (%)
100
50
0
0
10
20
30
40
50
Days after T cell transfer
no treatment
LMP2-rejT
CD19-CAR/HPV-rejT
DRrejT
D
LMP2-rejT
CD19-CAR/HPV-rejT
DRrejT
Tetramer+ CD3+ 0.41
Tetramer+ CD3+ 0.89
Tetramer, CD3 subset 2.42
CD3
tetramer (LMP2419-427)
tetramer (HPV16E649-57)
tetramer (LMP2419-427)
E
CAR copies / µg genomic DNA (log10)
1.E+07
1.E+06
1.E+05
1.E+04
1.E+03
1.E+02
1.E+01
1.E+00
****
Control
CD19-CAR/HPV-rejT
DRrejT